Journal of ELECTRONIC MATERIALS, Vol. 42, No. 6, 2013
DOI: 10.1007/s11664-013-2516-0

Transport Properties of Bulk Thermoelectrics: An International Round-Robin Study, Part II: Thermal Diffusivity, Specific Heat, and Thermal Conductivity

HSIN WANG,[1,11] WALLACE D. PORTER,[1] HARALD BÖTTNER,[2] JAN KÖNIG,[2] LIDONG CHEN,[3] SHENGQIANG BAI,[3] TERRY M. TRITT,[4] ALEX MAYOLET,[5] JAYANTHA SENAWIRATNE,[5] CHARLENE SMITH,[5] FRED HARRIS,[6] PATRICIA GILBERT,[7] JEFF SHARP,[7] JASON LO,[8] HOLGER KLEINKE,[9] and LASZLO KISS[10]

1.—Oak Ridge National Laboratory, Oak Ridge, TN, USA. 2.—Fraunhofer Institute for Physical Measurement Techniques, Freiburg, Germany. 3.—Shanghai Institute of Ceramics, Chinese Academy of Sciences, Shanghai, China. 4.—Clemson University, Clemson, SC, USA. 5.—Corning Inc., Corning, USA. 6.—ZT-Plus Inc., Azusa, CA, USA. 7.—Marlow Industries, Dallas, TX, USA. 8.—CANMET, Hamilton, ON, Canada. 9.—University of Waterloo, Waterloo, ON, Canada. 10.—University of Quebec at Chicoutimi, Chicoutimi, QC, Canada. 11.—e-mail: wangh2@ornl.gov

For bulk thermoelectrics, improvement of the figure of merit *ZT* to above 2 from the current values of 1.0 to 1.5 would enhance their competitiveness with alternative technologies. In recent years, the most significant improvements in *ZT* have mainly been due to successful reduction of thermal conductivity. However, thermal conductivity is difficult to measure directly at high temperatures. Combined measurements of thermal diffusivity, specific heat, and mass density are a widely used alternative to direct measurement of thermal conductivity. In this work, thermal conductivity is shown to be the factor in the calculation of *ZT* with the greatest measurement uncertainty. The International Energy Agency (IEA) group, under the implementing agreement for Advanced Materials for Transportation (AMT), has conducted two international round-robins since 2009. This paper, part II of our report on the international round-robin testing of transport properties of bulk bismuth telluride, focuses on thermal diffusivity, specific heat, and thermal conductivity measurements.

Key words: Thermoelectric, thermal conductivity, thermal diffusivity, specific heat, power factor, figure of merit

INTRODUCTION

In order to improve the figure of merit *ZT* of thermoelectrics, the most noticeable, recent advances have been in the reduction of thermal conductivity while maintaining the electrical properties. This is the case in both bulk and low-dimensional thermoelectrics.[1–5] In studies of bulk materials, skutterudites[6–10] and clathrates[11–14] are examples of Slack's[15] ideal thermoelectric material with phonon glass–electron crystal (PGEC) characteristics. More recent efforts have focused on nanocomposite materials,[16–22] in which nanosized precipitates or secondary phases play significant roles in scattering phonons and reducing lattice thermal conductivity. Materials processing techniques such as spark plasma sintering (SPS),[23–25] melt-spinning,[26–28] and high-energy ball milling[4,29,30] have resulted in significant improvements to many existing thermoelectrics. As a result, the maximum reported *ZT* values have increased from 1.0 to the range of 1.5 to 1.8 in recent years.

Successful decoupling of thermal transport and electronic transport properties is key to thermoelectric

(Received October 26, 2012; accepted January 21, 2013; published online March 13, 2013)

development. One implication of this development path is that the accuracy of thermal conductivity measurements is critical to the veracity of reported ZT values. However, thermal conductivities are often reported in the literature as final values without any detailed information as to how they were obtained. While no direct thermal conductivity measurements can be reliable above room temperature due to the large radiative heat loss and the lack of means to account for the heat loss accurately, thermal conductivity has been determined indirectly, calculated from the product of thermal diffusivity, specific heat, and density. Although the density of the material is easily measured well over temperatures below melting, it typically is not but is often regarded as constant with temperature. More accurate data are needed and can be obtained by taking the volume expansion into account. The two remaining properties to measure then are thermal diffusivity and specific heat capacity. Calculated thermal conductivity values are often reported without the corresponding diffusivity or specific heat data. As such, it is difficult for the community to discern the origin of large discrepancies in thermal conductivity values reported for similar materials.

In 2009, the participants in IEA-AMT annex VIII started an international effort on transport properties through round-robin testing. The first round-robin study on n- and p-type bismuth telluride was completed in May 2010. The second round-robin study on p-type bismuth telluride was carried out and completed in August 2011. Although the low-temperature National Institute of Standards and Technology (NIST) standard reference material (SRM) for Seebeck coefficient from 50 K to 395 K became available in October 2011,[31,32] there is no standard thermoelectric material available for thermal diffusivity or specific heat measurements. The only available reference materials are provided by instrument manufacturers as system validation and calibration references. These materials are usually Pyroceram 9606, Pyrex, iron, and copper for thermal diffusivity and molybdenum for specific heat. The current IEA-AMT study used n-type Bi_2Te_3 provided by Marlow Industries which had the same composition as that of the NIST SRM. It should be noted that the processing technique for this thermoelectric differed slightly from that of the SRM. Part II of this study focuses on thermal conductivity and the final evaluation of ZT.

THERMAL CONDUCTIVITY AND DIFFUSIVITY

Although thermal conductivity, k, is a steady-state property, it is closely linked to thermal diffusivity through Eq. (1),

$$k = 100 D \alpha C_p \left(\text{in W m}^{-1}\text{K}^{-1}\right), \tag{1}$$

where α is thermal diffusivity in cm^2/s, C_p is specific heat in J/gK, and D is density in g/cm^3. At low temperatures, i.e., 4 K to 200 K, it is possible to measure the thermal conductivity of a bulk specimen accurately from the definition of the Fourier equation:

$$\Delta Q/\Delta t = -kA\,\Delta T/\Delta x, \tag{2}$$

where k is thermal conductivity, A is the cross-section area, $\Delta Q/\Delta t$ is the rate of heat flow, and $\Delta T/\Delta x$ is the temperature gradient. This equation assumes a homogeneous material with one-dimensional (1-D) geometry between two measurement locations at constant temperature. While both commercial and home-made low-temperature thermal conductivity systems[33,34] are available, the common problem with low-temperature systems in measuring thermoelectrics is the difficulty in accounting for radiative heat loss from 200 K to 400 K.

Alternatively, the thermal diffusivity may be measured. Thermal diffusivity is a transient thermal transport property that quantifies a material's ability to spread heat over distance. Usually, the flash diffusivity method developed by Parker[35] is employed, using the one-dimensional heat flow equation[36] and a xenon flash lamp or laser to heat the front surface with a heat pulse. The ideal specimen is a thin disk with uniform thickness and no heat loss from the edges or sides. By solving the time-dependent temperature at the rear surface and using the known constants, thermal diffusivity is expressed in Parker's equation as

$$\alpha = 1.38 d^2/\pi t_{1/2}, \tag{3}$$

where only the sample thickness, d, and time for the back-surface temperature to reach half-maximum, $t_{1/2}$, are used to calculate the thermal diffusivity. The back-side temperature is usually measured using an infrared detector. Under a small temperature rise ($\Delta T < 5$ K), the detector output voltage has a linear dependence on temperature, allowing the back-surface temperature to be monitored using the detector voltage output alone (i.e., no absolute temperature measurement is necessary). When synchronized with the laser flash, $t_{1/2}$ can be determined. Accurate measurements of thickness and time are easier than the accurate temperature and heat flux measurements required by the steady-state method. Since Eq. (3) assumes no heat loss, it is often further modified for heat loss using the Clark and Taylor method[37] or the Cowan method[38] as described in ASTM E1461.[39] In commercial systems, it is common to perform a least-squares fit to the entire transient curve to obtain the thermal diffusivity.

SPECIFIC HEAT CAPACITY

Heat capacity is the amount of energy required to raise the temperature of a sample material by a certain amount and may be expressed in units of

J/K. Specific heat, C_p, is the heat capacity per unit mass under constant pressure. It is a temperature-dependent property of a material that is independent of microstructure. For normal crystalline solids, the Dulong–Petit law states that the specific heat under constant volume, C_v, is $3R$ per mole of atoms (where R is the universal gas constant). It should be noted that there is a difference between C_p and C_v:

$$C_p = C_v + (\mathrm{CTE})^2 T/\beta_T D, \tag{4}$$

where CTE is the coefficient of thermal expansion, β_T is the isothermal compressibility, and D is the density. If C_v approaches $3R$ at room temperature, the high-temperature C_p should be slightly higher than $3R$ and increasing with temperature. For bismuth telluride, $3R$ can be calculated using the known composition. For this study, the p-type material has a composition of $Bi_{0.5}Sb_{1.5}Te_3$. The total molar mass is 669.93 g/mol. The value of $3R$ (24.3 J/mol-K) is three times the gas constant value of 8.31 J/mol-K. Since there are a total of five atoms in the p-type formula, the Dulong–Petit limit is 0.186 J/g-K. The n-type material has a composition of $Bi_2Te_{2.7}Se_{0.3}$. The molar mass is 786.17 g/mol. With five atoms in the formula, the Dulong–Petit limit is 0.159 J/g-K. These values should be calculated if the actual composition of the material is known. The $3R \pm 5\%$ value at room temperature (the "$3R$ test") can be used as a guideline to judge the quality of measured C_p values.

Measurements of C_p were determined by the heat flow method using a Quantum Design physical properties measurement system (PPMS). Low-temperature grease is used in the "C_p mode" from 2 K to 200 K. From 200 K up to 400 K, high-temperature grease is often used for the best results. At even higher temperatures of 300 K to 1000 K, C_p was measured b differential scanning calorimeter (DSC) following ASTM standard E1296, wherein three separate runs *must* be performed: empty pan run, sapphire run, and sample run. For bismuth telluride (from 300 K to 500 K), the measurement temperature range for C_p is small, and the C_p rate of change is small. A slight change in the instrument baseline could result in a large change in C_p. Therefore, it is always advisable to test the materials at room temperature and below when possible (Fig. 1). If C_p is measured using a low-temperature and a high-temperature system separately, the C_p data over the entire temperature range should be used to generate a Debye function-based curve fit, because neither the low-temperature ($T < 300$ K) nor the high-temperature ($T > 300$ K) data alone are sufficient to produce a good curve fit for the entire temperature range. Figure 1 shows experimental data obtained at Oak Ridge National Laboratory (ORNL) on Marlow's bismuth telluride alloys, which have similar compositions to those of the round-robin materials. The solid lines are Debye model-based curve fits. The Debye function for specific heat is used as C_v for all samples:

$$C_v = 9nR\left(\frac{T}{\theta_\mathrm{D}}\right)^3 \int_0^{\theta_\mathrm{D}/T} \frac{x^4 e^x}{(e^x - 1)^2} dx, \tag{5}$$

where θ_D is the Debye temperature and R is the universal gas constant. At low temperatures ($T << \theta_\mathrm{D}$), Eq. (5) follows the Debye T^3 law, and it becomes the Dulong–Petit limit of $3R$ at $T >> \theta_\mathrm{D}$. $C_v/3R$ is the Debye function and can be approximated by a ninth-order polynomial using the calculated C_v values according to Gopal[40], as

$$C_v/3nR = D(T, \theta_\mathrm{D}, n) = 1 + d_1(\theta_\mathrm{D}/T) + d_2(\theta_\mathrm{D}/T)^2 + \cdots + d_9(\theta_\mathrm{D}/T)^9, \tag{6}$$

in which temperature T, Debye temperature θ_D, and atoms per unit formula n are variables. We combine both high-temperature and low-temperature data and use a physical curve fit model by assuming $C_p \approx C_v$ in Eq. (7) and substitute it into the Nernst–Lindemann relation based on Grüneisen's equation of state,[40]

$$C_p \approx C_v + AC_p^2 T. \tag{7}$$

Parameter A is nearly constant over a wide temperature range from 100 K to 1000 K. We have

$$C_p = [D(T, \theta_\mathrm{D}, n) + AD(T, \theta_\mathrm{D}, n)^2 T]/M. \tag{8}$$

The nine parameters found in Eq. (6) are passed to Eq. (8), and θ_D, M (molecular weight), and A are used as new curve-fitting parameters to obtain the Debye temperature. In most cases, A is a constant and M is known or can be approximated using the composition of the material. As an example, Eq. (8) was used to fit the experimental data of both n- and

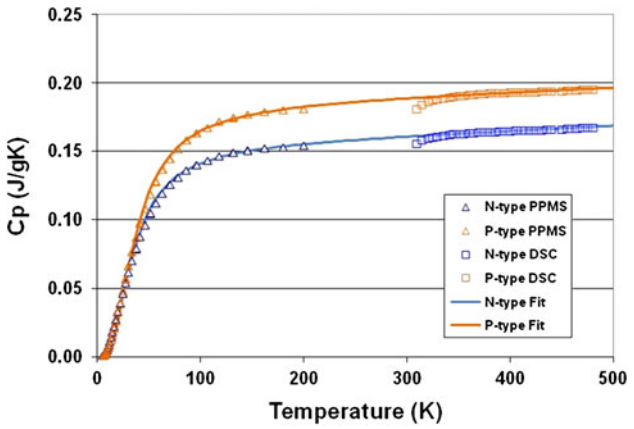

Fig. 1. Specific heat of n-type and p-type thermoelectric alloys measured by PPMS from 10 K to 200 K, DSC from 300 K to 500 K, along with curve fits. The fitting correlation coefficients were >0.995.

p-type bismuth telluride materials between 4 K and 500 K in Fig. 1. The Debye temperature θ_D value of the *n*-type material is 140 K, and for the *p*-type material it is 152 K. For this work, the main purpose of full-temperature-range curve fitting is to evaluate whether the common practice of only measuring high-temperature C_p has sufficient accuracy for thermal conductivity calculation.

MEASUREMENT SYSTEMS AND MATERIALS USED IN ROUND-ROBIN

In the round-robin study, two measurement systems were used by participating laboratories for thermal diffusivity:

- Netzsch LFA447 and LFA457
- TA Instrument/Anter Flashline5000 and XPlatform

Three types of commercial differential scanning calorimeter (DSC) systems were used for specific heat:

- Netzsch DSC
- TA Instrument DSC
- Quantum Design physical properties measurement system (PPMS)

The basic round-robin rules were set as follows:

(1) Each laboratory should use its normal practice to test the samples and report the results;
(2) No laboratory will be identified in the reports;
(3) The purpose of the round-robin is to identify testing issues, not to rank laboratory performance;
(4) Round-robin data analysis may require system calibration data. Failure to provide system calibration could result in the data not being included in the combined results.

In order to measure thermal conductivity, eight sets of specimens for both *n*-type Bi_2Te_3 and *p*-type Bi_2Te_3-Sb_2Te_3 alloy were prepared (four samples per set). Figure 2 shows one set of IEA-AMT specimens for specific heat and thermal diffusivity measurements. The specimens were prepared and machined to specifications by Marlow Industries.

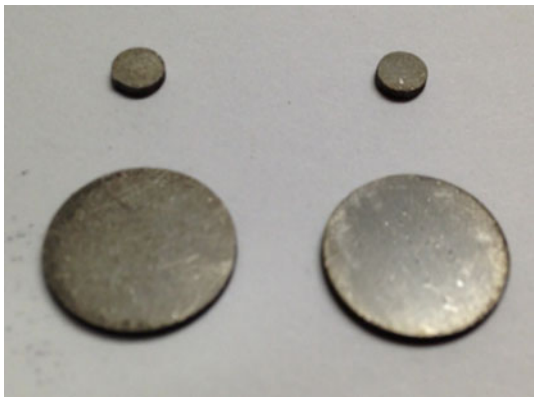

Fig. 2. Round-robin 1 samples sent to each laboratory: two *p*-type (left) and two *n*-type (right) samples.

First International Round-Robin

One set of round-robin specimens was sent to each laboratory with the same instructions. No instructions for testing procedures were given, and each laboratory was asked to perform the tests using their best practice. Each laboratory was asked to measure these samples to a maximum temperature of 502 K starting from room temperature. Specifically, the following instructions were sent to each laboratory for testing:

Thermal Diffusivity from 300 K to 502 *K*

Use the 1-mm-thick × 12.7-mm-diameter disk. Describe instrument used. Report the following parameters: actual sample thickness used, sample holder material and geometry. Record the following measurement parameters: test atmosphere, laser or flash lamp power. Record and save the raw transients. Analysis must include a pulse width correction and the calculation of the diffusivity using Cowan, Clark & Taylor, Koski or nonlinear least-squares curve fitting.

Specific Heat from 300 K to 502 K

Use 1 mm thick x 4 mm diameter disk. Describe equipment used. For DSC, report parameters: sample weight, sample pan material, reference material (geometry and weight). Record the following measurements: raw data for empty pan (baseline), reference and sample runs, test atmosphere, heating/cooling rate. Analyze data in accordance with ASTM E1296 "three-run" C_p calculation.

All participating laboratories performed thermal diffusivity measurements, and only one laboratory could not perform C_p measurements in the first round-robin. In the following discussion, the laboratory identification numbers are not the same in each section. The laboratory identities were intentionally mixed because the main purpose of the round-robin was not to rank the performance of each laboratory but rather to identify all the issues related to transport properties of bulk thermoelectrics.

Thermal Diffusivity

The thermal diffusivity results from seven laboratories are shown in Fig. 3. All the laboratories used the laser flash method. The two most common commercial systems used were made by Anter Corporation (now TA Instruments) and Netzsch. The data for *n*-type materials are plotted as solid symbols and for *p*-type materials as unfilled symbols of the same color. The raw data from each laboratory represented average values of at least three measurements per temperature. The scatter at room temperature was about ±2% to ±3%, and the largest scatter of ±6% to ±10% occurred at high temperatures for both *p*- and *n*-type materials. While ASTM E1461 for flash diffusivity calls for analysis

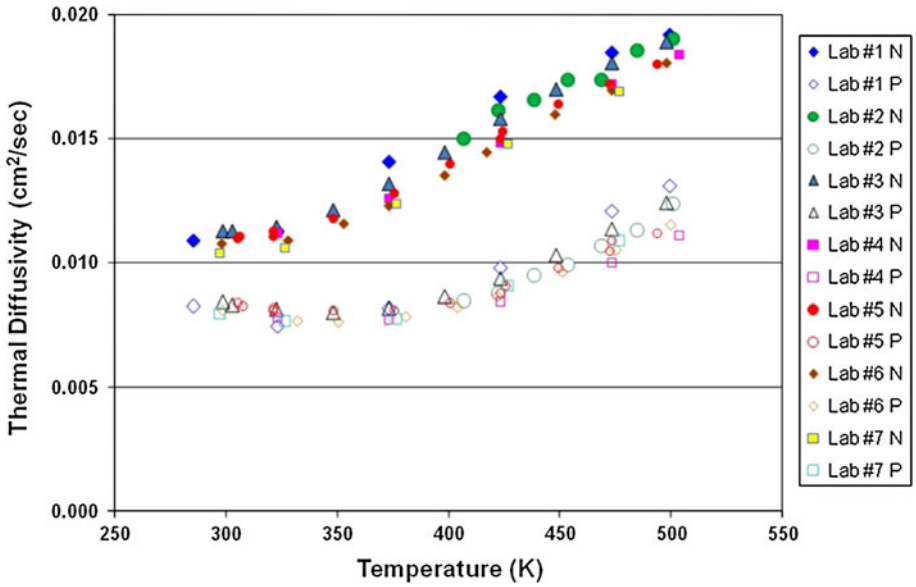

Fig. 3. Thermal diffusivity results of round-robin 1 from seven laboratories. *n*-type: filled symbols; *p*-type: unfilled symbols.

using the Clark and Taylor method, the data analysis by each laboratory varied. Several laboratories used the Cowan analysis. Although the original ASTM E1461 recommended limited numbers of data points to be used, the latest laser flash software utilizes the entire curve to calculate diffusivity. Thus, no particular analysis was recommended to present the results. The overall results for thermal diffusivity were consistent among the seven laboratories. Scatter in the diffusivity values was expected, given that the measurement accuracy of commercial laser flash systems is usually ±6% to ±8%. The results of several laboratories using both Cowan or Clark and Taylor analysis showed much smaller variations than the scatter.

Specific Heat

The specific heat results from six laboratories are shown in Fig. 4 with the curves from Fig. 1 replicated for reference. All the laboratories used the differential scanning calorimeter (DSC) method. One laboratory performed the tests using two types of DSC, and the heating and cooling data are both presented. As mentioned before, in DSC measurements, the Dulong–Petit limit (3*R* test) should be used as a guideline for the measured values. Three quality criteria need to be followed for high-temperature C_p measurements:

(1) C_p should be within ±5% at $T \geq 300$ K;
(2) C_p should be slightly higher than C_v;
(3) Due to thermal expansion, C_p should increase slightly at higher temperatures.

Even without the low-temperature curve-fit results, the 3*R* test can be used to verify C_p results near or above room temperature.

Initially, the DSC results showed very large discrepancies among the six laboratories and that the above three criteria were ignored in some cases. The results from two laboratories (Lab #1 and #3, shown in rectangular boxes in Fig. 4) were obviously wrong, showing 40% to 50% or even higher variations compared with expected C_p values. They completely failed the 3*R* test, and the materials must be remeasured. One of the most important things to check is the agreement of the heating and the cooling curves. If the two curves are not equivalent, this is an indication of instrument baseline shift. A new baseline must be run in order to obtain correct C_p values. When the C_p data from Labs #1 and #3 are removed from Fig. 4, the scatter among other datasets was about ±4%, showing reasonably good agreement among the remaining four laboratories. After the first round-robin, a document was prepared for DSC operators to fill out and answer to ensure the proper procedures were followed, as a necessary step towards developing standard procedures.

Summary of Round-Robin 1

The first round-robin among seven laboratories using the Marlow Bi_2Te_3 alloys was completed within 4 months. The study achieved its original goal, i.e., to identify measurement problems for bulk transport properties. After testing the commercially available materials within a moderate temperature range, the IEA-AMT annex study observed the following:

1. Thermal diffusivity measurements by laser flash give about ±6% to ±8% scatter. The test results could be better if the ASTM E1461 data analysis procedure were to be followed.
2. Specific heat measurements show large scatter, despite the existence of ASTM standard E1296

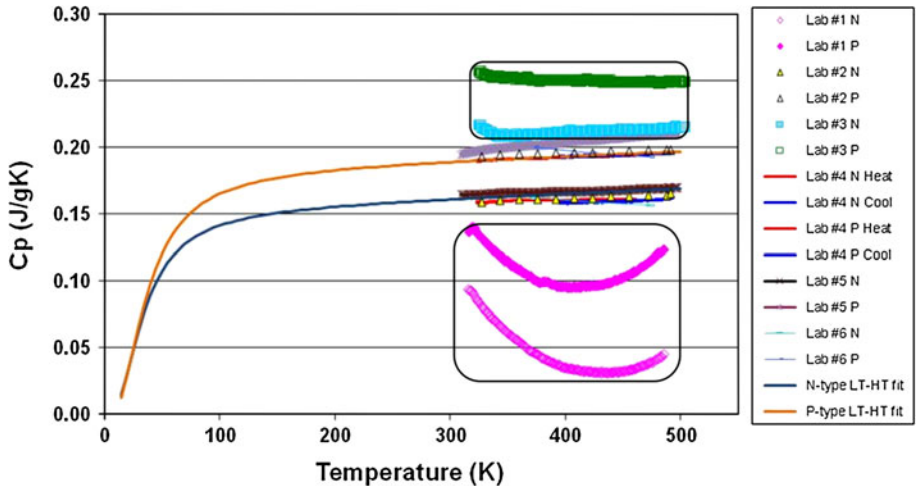

Fig. 4. Specific heat results of round-robin 1 from six laboratories. Lab #1 and #3 results, shown in the boxes, failed the 3*R* test.

for the DSC method. The largest errors occur when the baseline of the instrument shifted during reference, empty pan, and sample runs. When obvious mistakes due to lack of operator experience were eliminated, the measured C_p data showed a scatter of ±4%.

The round-robin 1 test used nonproduction Marlow Bi_2Te_3 materials. Although they are known to have rather consistent properties, it is still possible to have scatter due to localized material nonuniformity. Since each laboratory received a separate set of specimens, the possibility of variations among the materials did exist. To understand the uniformity of the materials, groups of 12 *n*- and *p*-type Marlow materials were selected and tested at room temperature at ORNL with a TA/Anter X-platform xenon flash system. This room-temperature system has a 24-sample carousel and used an intrinsic contact thermocouple to detect temperature rise. Figure 5 shows room-temperature thermal diffusivity results of 12 *n*- and 12 *p*-type samples. The specimens are 12.7-mm-diameter × 1-mm-thick disks from the same batch as the IEA-AMT round-robin materials. The standard deviations were ±1.54% for the *p*-type materials and ±2.75% for the *n*-type materials. Similar to the electrical resistivity results, the *p*-type material showed better sample-to-sample consistency and was therefore selected for a second round-robin study.

SECOND INTERNATIONAL ROUND-ROBIN

The second round-robin testing began in August 2010 and was completed by August 2011. Two sets of *p*-type materials were measured at seven laboratories in four countries. The results of round-robin 1 were given to all the laboratories as reference. The issues identified in round-robin 1 were discussed by the participating laboratories. The same test instruments used for round-robin 1 were again used for round-robin 2, with all the laboratories completing testing on all specimens. In some cases, thermal diffusivity and C_p testing were carried out at different laboratories within the same country.

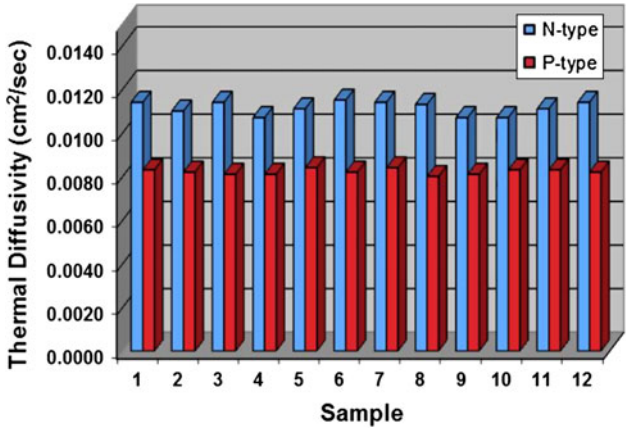

Fig. 5. Thermal diffusivity of 12 *n*-type and 12 *p*-type samples at room temperature.

Thermal Diffusivity

The thermal diffusivity results from seven laboratories are shown in Fig. 6. All the laboratories used a laser flash system made by either the Anter Corporation or Netzsch. The two *p*-type specimens, circulated in opposite directions among the laboratories, were measured separately in some cases a few months apart. Except for one measurement by Lab #6, the scatter at room temperature was about ±4% to ±6%. The greatest scatter of ±15% to ±17% was observed at 473 K, which was larger than that in round-robin 1. Since the same materials were passed around, the sample-to-sample variations were minimized. One laboratory used a cryogenic temperature system to measure the diffusivity down to 123 K. Those data agreed well with the laboratory averages

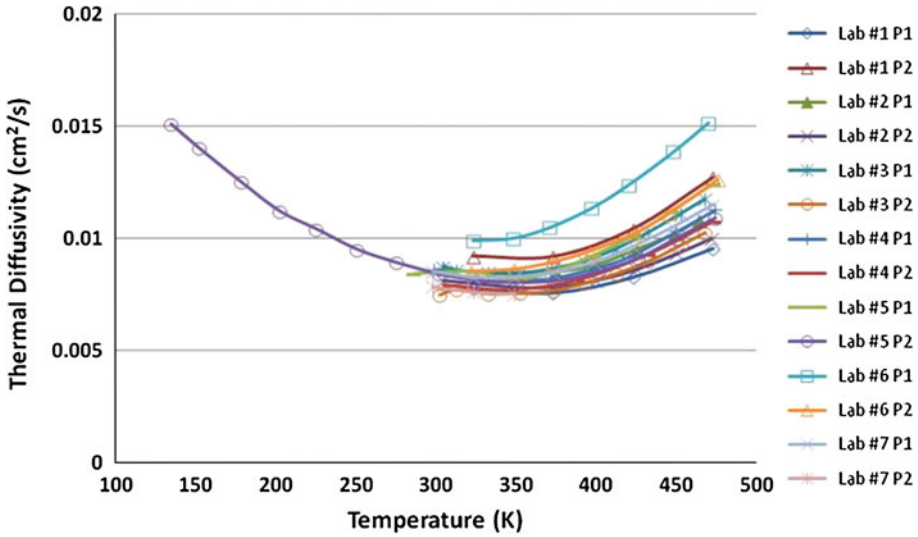

Fig. 6. Thermal diffusivity results of round-robin 2 from seven laboratories.

and provided a larger trend of diffusivity versus temperature. It was found that in some cases the thickness measurements of a particular specimen deviated by 5% to 6% among different laboratories. Since thickness is the only input parameter used in calculation of thermal diffusivity, this uncertainty alone could be a major source of error, as a 1% error in thickness can result in a 2% error in thermal diffusivity. Although most laboratories used a digital micrometer and have a metrology program to calibrate the micrometers, the practice of measuring a reference thickness was not widely adopted. Thickness error could be caused by low battery power and/or lack of calibration against a standard after every measurement. Possible instrument variations were observed. Several laboratories using TA Instrument/Anter systems reported higher values than the laboratories using the Netzsch systems despite similar analysis techniques.

Specific Heat

The specific heat results from seven laboratories are shown in Fig. 7. Although specific guidelines were sent to the laboratories, DSC measurements continued to present the biggest challenge. More than ±15% scatter was observed in the combined data. While in most cases the test procedure was followed, the nature of DSC measurements, i.e., that three separate runs must be taken to calculate C_p, made this test the most difficult one to be reproducible. In the most common DSC systems, baseline change is common and cannot be controlled by the operator. The best practice then is to run a baseline and reference run, record heating and cooling data on the test specimen, and run the baseline again. If the baseline shifts substantially (more than 2%), the test must be repeated. C_p should be determined for the molybdenum NIST standard to check the accuracy of the instrument periodically. In some cases, variation can be identified; For example, the results from Lab #2 in Fig. 7 show a significant "hook" at the beginning of the run. This is usually caused by a mismatch in mass or size of the reference sample. The DSC signals of the reference sample should match the test sample in magnitude and shape as closely as possible. A good practice is to choose a reference (sapphire) that gives a signal similar to the sample rather than using the same reference for all measurements. There were also four cases of uncorrected baseline shifts that resulted in larger than 5% room-temperature deviations from the Dulong–Petit limit of 0.186 J/gK.

Summary of Round-Robin 2

The second round-robin among seven laboratories using the Marlow p-type Bi_2Te_3-Sb_2Te_3 alloy was completed within 12 months. By measuring the same specimens, differences introduced by sample-to-sample variations were minimized. However, measurement issues still existed. In some cases the data showed larger scatter than in the first round-robin. It was found that:

1. Thermal diffusivity of p-type materials showed ±6.8% scatter at room temperature and ±17% scatter at 475 K (except for one sample from one laboratory).
2. Specific heat showed more than ±15% scatter in the temperature range. Half of the laboratories could measure with ±5% scatter, as per a check using the Dulong–Petit limit. Results from some laboratories still showed lack of checking for uncorrected baseline shifts and/or standards use. This study revealed that the DSC measurement is the most operator dependent and is very likely to produce unreliable results.

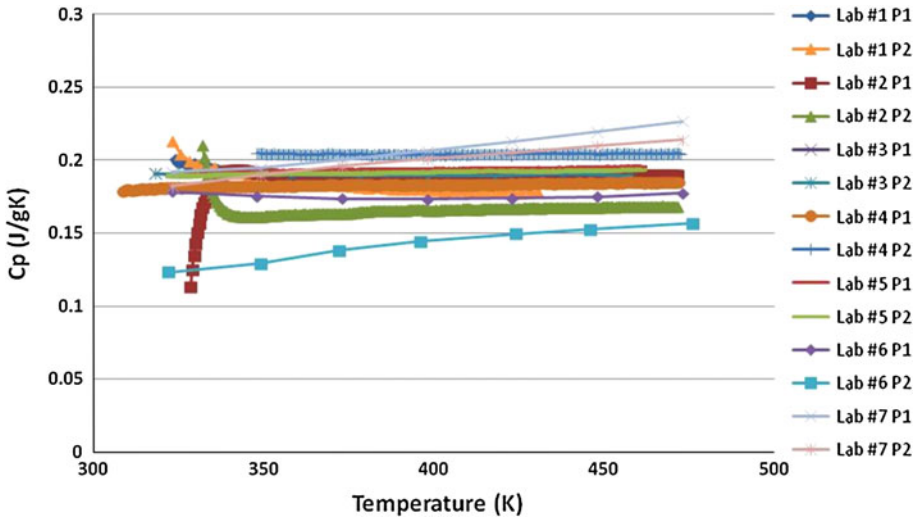

Fig. 7. Specific heat results of round-robin 2 from seven laboratories on 14 samples.

FIGURE OF MERIT CALCULATION AND TEST PROCEDURE

The results of the second international round-robin were analyzed to produce summarized results on thermal diffusivity and specific heat. Since the actual temperatures of each set of results are scattered, all the data points for thermal diffusivity were plotted as a pool as shown in Fig. 8. The Lab #6 P2 data were dropped because there was no system calibration given to show that the apparent variation at every temperature was valid. For the thermal diffusivity of p-type bismuth telluride, a third-power polynomial curve fit was used to represent the temperature range from 293 K to 475 K:

$$\alpha = -1 \times 10^{-10}T^3 + 3 \times 10^{-7}T^2 - 0.0002T + 0.0362 \ (\mathrm{cm}^2/\mathrm{s}), \quad (9)$$

where T is temperature in Kelvin. The data scatter over Eq. (9) is ±6.8% near room temperature and ±17.1% at 475 K.

The scatter for specific heat data over the entire temperature range was ±5%, after removing data that failed the $3R$ test and some initial data from one laboratory due to obvious lack of isothermal hold and sample–reference mass mismatch. To improve the curve fitting, a low-temperature and high-temperature C_p measurement were conducted on similar Marlow materials, and Eqs. (5) and (6) were used to curve-fit the data obtained from PPMS and DSC (Fig. 9). The power factor (PF = S^2/ρ) was calculated using the Seebeck coefficient, S, and electrical resistivity, ρ, from all the laboratories in part I of this study[44] and is presented in the scatter plot. A linear curve-fit is used to represent the average values (Fig. 10). The average density of p-type bismuth telluride was determined from five thermal diffusivity disks to be 6.767 g/cm^3 with ±0.4% scatter. Thermal conductivity, k, was calculated

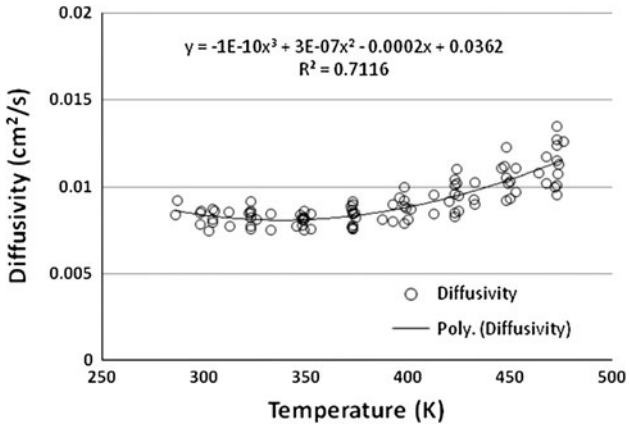

Fig. 8. Scattered data plot and curve fitting of thermal diffusivity.

using Eq. (1), and the figure of merit, ZT, was calculated using

$$ZT = \mathrm{PF} \times T/k. \quad (10)$$

An uncertainty analysis was conducted using the standard error analysis and propagation method and provided an overestimation of possible experimental errors among the laboratories, since reported standard deviations were usually smaller. The data variation for eight selected temperatures was used in the analysis, and the uncertainties are presented in Table I. The uncertainty of thermal conductivity, k, is $\delta_k = (\delta_D^2 + \delta_{Cp}^2 + \delta_\alpha^2)^{0.5}$ and for ZT, $\delta_{ZT} = (\delta_T^2 + \delta_{PF}^2 + \delta_k^2)^{0.5}$. The measurement uncertainties for density, D, temperature T, and C_p are assumed to be independent of temperature.

ZT and thermal conductivity are plotted as a function of temperature in Fig. 11, with uncertainties calculated in Table I plotted as error bars for eight temperatures. Because of the large scatter in thermal diffusivity, the uncertainties for thermal

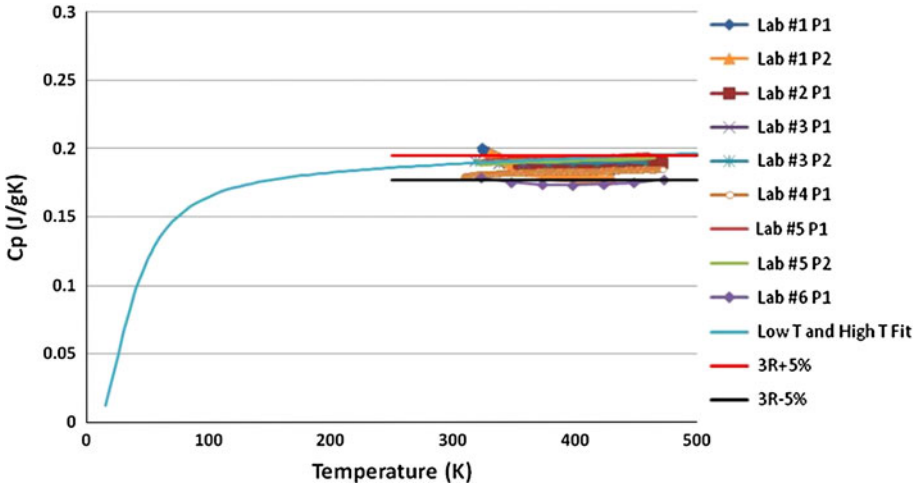

Fig. 9. C_p data after filtering with the 3R test, along with p-type curve fit shown in Fig. 1.

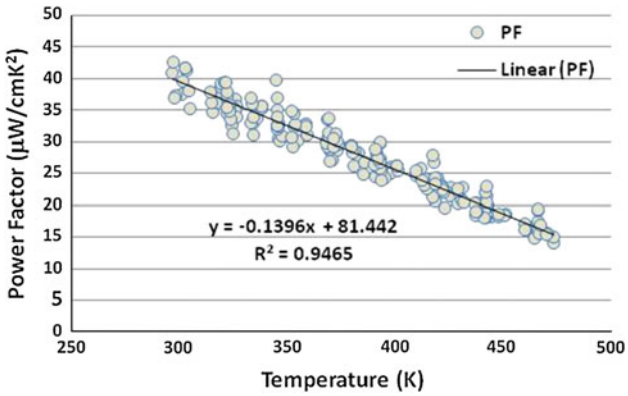

Fig. 10. Power factor calculated from Seebeck coefficient and electrical resistivity, measured by all the laboratories in round-robin 2.

conductivity were estimated at ±9.2% at 300 K and ±17.9% at 475 K. The overall scatters for ZT were estimated at ±11.7% at 300 K and ±20.9% at 475 K. We believe that, by following proper testing procedures suggested by these round-robin results, it is possible to achieve <±10% experimental uncertainty of ZT.

The main purpose of this IEA-AMT study is to identify transport measurement issues and develop standard test procedures. The international round-robin studies showed that the calculated thermal conductivity from measured density, thermal diffusivity, and specific heat is the biggest source of error for thermoelectric figure of merit. In order to improve thermal conductivity measurements, a recommended test procedure for thermal diffusivity and C_p has been drafted by the participants.

Test Procedure for Thermal Diffusivity

Specimen

The standard thermal diffusivity specimen should be a thin disk or plate. For most commercial equipment, the standard specimen is a 12.7-mm-diameter disk. The thickness of the disk is determined by the thermal diffusivity values of the material. In general, the diameter of the specimen should be at least four to five times larger than its thickness. A larger diameter-to-thickness ratio ensures that the one-dimensional heat flow assumption is valid. If the thickness is comparable to the diameter, heat loss from the side of the specimen will cause measurement errors. For thermoelectric materials with thermal conductivity of 1 W/mK to 3 W/mK, the thickness of the 12.7-mm-diameter specimen is optimally 1 mm, making the diameter-to-thickness ratio about 13:1.

The most important aspect of specimen preparation is to achieve parallel surfaces, since the thickness is the only parameter to be entered during the thermal diffusivity test. The accuracy of the thickness will directly affect the accuracy of the thermal diffusivity. While the surfaces need to be flat, polishing is not required as a mirror-like surface finish will reflect the heat pulse (laser or xenon flash light) and present low emissivity for the infrared detectors. To ensure consistent surface conditions, it is a common practice to spray a thin layer of graphite onto both sides of the specimen. For materials that are translucent or transparent, a thin layer of metal coating (or graphite coating) is required. Commercial laser flash systems usually employ a YAG laser (1.06 μm wavelength) and InSb infrared detector (3 μm to 5 μm). It is important to ensure that the specimen is not transparent to these infrared (IR) wavelengths; For example, silicon is highly transparent in the IR region and so requires metal or graphite coating.

Thermal Diffusivity Test

Thermal diffusivity testing is a time-domain transient method. There is no need to measure specimen temperature, as long as the temperature rise of the specimen is small. The half-rise time, i.e., the time to reach half-maximum temperature

Table I. Round-robin uncertainties based on data scatter (maximum scatter from the mean value divided by the mean value)

T (K)	δ_D	δ_{Cp}	δ_α	δ_k	δ_{PF}	δ_T	δ_{ZT}
300	0.004	0.050	0.172	0.092	0.071	0.010	0.117
325	0.004	0.050	0.144	0.108	0.117	0.010	0.159
350	0.004	0.050	0.142	0.085	0.088	0.010	0.122
375	0.004	0.050	0.117	0.108	0.111	0.010	0.155
400	0.004	0.050	0.096	0.128	0.093	0.010	0.158
425	0.004	0.050	0.068	0.151	0.077	0.010	0.170
450	0.004	0.050	0.095	0.153	0.080	0.010	0.173
475	0.004	0.050	0.078	0.179	0.108	0.010	0.209

The uncertainties for density, C_p, and temperature are assumed to be constant over the temperature range.

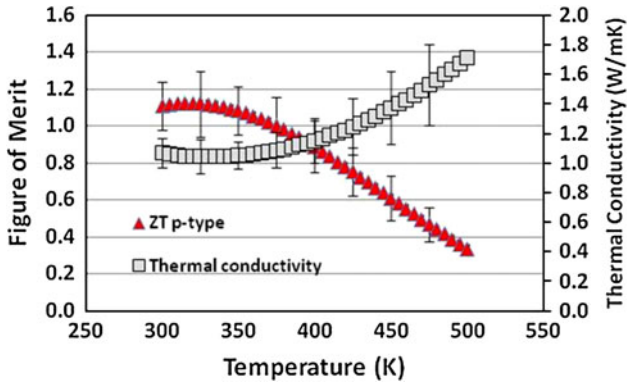

Fig. 11. Calculated figure of merit, *ZT*, and thermal conductivity for *p*-type Bi_2Te_3.

(expressed in detector voltage), is measured from the back of the specimen.

Laser power: The laser power should be enough to raise the back-surface temperature by 1 K to 5 K. In general, a 1 V to 2 V signal from the IR detector with low noise is sufficient. In some systems, the laser power can be adjusted by the software. It is important to know that the IR detector is not sensitive at room temperature, but its sensitivity increases exponentially as temperature increases.

Data collection time: Commercial systems either collect data for a fixed length of time (12 s) or try to adjust optimal data collection times after determining the peak position following the first shot. A usual rule-of-thumb is to keep the time to detect the peak detector voltage within 2 s after the heat pulse. If it takes longer than 2 s to reach maximum temperature, this is an indication that the specimen should be thinner. For low-thermal-conductivity materials, it is important to wait a sufficiently long time between heat pulses to allow the specimen to cool down.

Number of measurements: At least three measurements are needed for each specimen at each set point.

Calibration and references: To qualify the accuracy of the flash diffusivity system, several standards are used such as Poco graphite or thermal graphite, Pyroceram 9606, Pyrex, stainless steel or alumina. For thermoelectric materials, Pyroceram 9606 should be used because it has similar thermal diffusivity and thermal conductivity. If it is not available, stainless-steel or alumina references can be used. Periodic calibration runs are necessary to show that the system is operating within designed specification when the test is performed.

Data Analysis

Thermal diffusivity calculation is based on a one-dimensional heat flow model. The simplest calculation is under the adiabatic condition, i.e., the Parker method, Eq. (3). In reality, the specimen will have heat loss, and the laser or xenon flash pulse width will need to be corrected. In ASTM E1461 for the flash method, calculation to correct the constant in the Parker equation is recommended. ASTM E1461 also recommends the Clark and Taylor (ratio) method and the Cowan method. Other calculation methods such as the Koski,[41] Heckman,[42] and Cape and Lehman[43] methods are frequently used. Some of these methods were developed for specific materials or specific conditions. When using a given method, it is important to understand the specific conditions that apply to the method, i.e., very high or low thermal conductivity, transparent materials, inhomogeneous materials, etc. For thermoelectrics with thermal conductivities of 1 W/mK to 5 W/mK and which are opaque in the visible and IR ranges, it is the advice of IEA-AMT to use the Clark and Taylor or Cowan method with pulse width correction as suggested in ASTM E1461.

Reporting

Thermal diffusivity values calculated by the Clark and Taylor or Cowan method need to be reported along with the specimen geometry, laser power, and data collection time. Diffusivity data from multiple tests should be reported, and the standard deviation calculated as a measure of

repeatability. Test results of periodic calibrations of the system using reference materials need to be available. The raw data transients need to be examined for signal quality and saved.

Test Procedure for Specific Heat

Specimen

The standard specific heat specimen for differential scanning calorimeter (DSC) should be a thin disk, 4 mm to 6 mm in diameter and about 1 mm thick, depending on the measurement system selected. The specimen needs to be flat and have the total heat capacity close to that of the reference material. Powders, broken pieces or specimens having different geometries will have different heat transfer characteristics from the reference sample and will introduce measurement errors. Descriptions of specimen holders/pans/lids including material, geometry, dimensions, mass, and venting or sealing method need to be recorded.

DSC Measurements and Data Analysis

The DSC method to determine specific heat is described in ASTM standard E1296 and ISO 11357 and requires three separate scans: an empty pan (baseline scan), a scan using a sapphire standard, and a sample scan. A typical DSC test should include both a heating scan and a cooling scan. After testing, it is highly recommended to run another baseline scan, especially when the heating and cooling curves show significant shifts ($>2\%$ change).

When performing the DSC measurements and data analysis, the following descriptions are needed:

1. Calorimeter mode: DSC-Standard Ramp, DSC-Step, DSC-Modulated Ramp, DSC-Modulated Quasi-isothermal, or other.
2. Specify sensor type/model and provide a description (include diagram) of sensor thermocouple placement, type (separate four-wire, differential three-wire, thermopile, etc.), and the thermocouple material/type.
3. Description of data analysis software including name and version number. If any baseline drift corrections were used, describe algorithm used.
4. Description of pretest procedure including vacuum/purge cycles, vacuum bake-out/degassing, purge gas type, purity, and flow rate. If sealed lids were used, include atmospheric conditions under which the pans were sealed.
5. Description of standard reference material used for heat flow calibration including material, geometry, dimensions, mass, and any traceability to a national standards organization.
6. Description of test procedure including any standard test method followed (ASTM, ISO, DIN, etc.), starting and ending temperatures, temperature and duration of any isothermal segments, heating/cooling rates used, and period and amplitude if using modulated techniques. Note specifically if a "single-run" method using a stored instrument calorimetric calibration was used to calculate the heat capacity data.
7. Description of any recently obtained heat capacity results, including error plot, on a reference material traceable to a national standards organization, or results on a material with well-known heat capacity values that were used to determine the accuracy of the instrument and test procedure used. Materials used for this check should be different from that used as the standard reference material for the current measurements. (Example: Do not test a sapphire specimen as an accuracy test if sapphire is your reference material.)
8. Description of temperature scale calibration including method, materials used, frequency, last calibration date, etc.

CONCLUSIONS

The international round-robin study by IEA-AMT is a timely effort to help enable the commercialization of thermoelectric devices, especially for automotive applications. Using hot-pressed *n*- and *p*-type bismuth telluride materials from Marlow Industries, major measurement issues for thermal diffusivity and specific heat have been identified. In some cases, the measurement results were not acceptable. We identified the critical issues of specific heat measurement errors and the lack of reporting of specific heat in the literature. Thermal conductivity has been the most noticeable contributor to ZT improvement, but is also the most unreliably measured of the three transport properties, i.e., thermal conductivity, Seebeck coefficient, and electrical resistivity. Detailed test procedures have been developed for both thermal diffusivity and specific heat measurements to improve their accuracy and reliability.

ACKNOWLEDGEMENTS

The authors would like to thank the International Energy Agency under the Implementing Agreement for Advanced Materials for Transportation for supporting this work and the assistant secretary for Energy Efficiency and Renewable Energy of the Department of Energy and the Propulsion Materials Program under the Vehicle Technologies Program. We would like to acknowledge support from all participating institutions and Oak Ridge National Laboratory managed by UT-Battelle LLC under contract DE-AC05000OR22725.

REFERENCES

1. R. Venkatasubramanian, E. Siivola, T. Colpitts, and B. O'Quinn, *Nature* 413, 597 (2001).
2. K.F. Hsu, S. Loo, F. Guo, W. Chen, J.S. Dyck, C. Uher, T. Hogan, E.K. Polychroniadis, and M.G. Kanatzidis, *Science* 303, 818 (2004).

3. T. Caillat, J.-P. Fleurial, and A. Borshchevsky, *J. Phys. Chem. Solids* 58, 1119 (1997).
4. B. Poudel, Q. Hao, Y. Ma, Y. Lan, A. Minnich, B. Yu, X. Yan, D. Wang, A. Muto, D. Vashaee, X. Chen, J. Liu, M.S. Dresselhaus, G. Chen, and Z. Ren, *Science* 320, 634 (2008).
5. P. Kim, L. Shi, A. Majumdar, and P.L. McEuen, *Phys. Rev. Lett.* 87, 215502 (2001).
6. G.S. Nolas, G.A. Slack, and S.B. Schujman, *Semicond. Semimet.* 69, 255 (2000).
7. B.C. Sales, D. Mandrus, and R.K. Williams, *Science* 272, 1325 (1996).
8. G.S. Nolas, M. Kaeser, R.T. Littletonand, and T.M. Tritt, *Appl. Phys. Lett.* 77, 1855 (2000).
9. D.T. Morelli and G.P. Meisner, *J. Appl. Phys.* 77, 3777 (1995).
10. C. Uher, *Semicond. Semimet.* 69, 139 (2000).
11. V.L. Kuznetsov, L.A. Kuznetsova, A.E. Kaliazin, and D.M. Rowe, *J. Appl. Phys.* 87, 7871 (2000).
12. J. Martin, G.S. Nolas, H. Wang, and J. Yang, *J. Appl. Phys.* 102, 103719 (2007).
13. W. Jeischko, *Metall. Trans. A* 1A, 3159 (1970).
14. S.J. Poon, ed. T.M. Tritt, *Semiconductors and Semimetals*, Vol. 70, Chap. 2, eds., R.K. Willardson and E.R. Weber (Academic, New York, 2001), p. 37.
15. G.A. Slack, *CRC Handbook of Thermoelectrics*, ed. D.M. Rowe (CRC, Boca Raton, FL, 1995), pp. 407.
16. D. J. Singh, *Sci. Advan. Mater.* 3, Special Issue: SI, 561 (2011).
17. J.F. Li, W.S. Liu, L.D. Zhao, and M. Zhou, *NPG Asia Mater.* 2, 152 (2010).
18. G.S. Nolas, J. Poon, and M. Kanatzidis, *Mater. Bull.* 31, 199 (2006).
19. A.J. Minnich, M.S. Dresselhaus, Z.F. Ren, and G. Chen, *Energy Environ. Sci.* 2, 466 (2009).
20. Y.Q. Cao, X.B. Zhao, T.J. Zhu, X.B. Zhang, and J.P. Tu, *Appl. Phys. Lett.* 92, 143106 (2008).
21. S.F. Fan, J.N. Zhao, J. Guo, Q.Y. Yan, J. Ma, and H.H. Hng, *Appl. Phys. Lett.* 96, 182104 (2010).
22. G. Joshi, X. Yan, H.Z. Wang, W.S. Liu, G. Chen, and G.Z.F. Ren, *Adv. Energy Mater.* 1, 643 (2011).
23. M. Zhou, J.F. Li, and T. Kita, *J. Am. Chem. Soc.* 130, 4527 (2008).
24. I. Matsubara, R. Funahashi, T. Takeuchi, and S. Sodeoka, *J. Appl. Phys.* 90, 462 (2001).
25. Y.H. Liu, Y.H. Lin, Z. Shi, C.W. Nan, and Z. Shen, *J. Am. Ceram. Soc.* 88, 1337 (2005).
26. W.J. Xie, X.F. Tang, Y.G. Yan, Q.J. Zhang, and T.M. Tritt, *Appl. Phys. Lett.* 94, 102111 (2009).
27. X.F. Tang, W.J. Xie, H. Li, W.Y. Zhao, Q.J. Zhang, and M. Niino, *Appl. Phys. Lett.* 90, 012102 (2007).
28. H. Li, X.F. Tang, X. Su, Q.J. Zhang, and C. Uher, *J. Phys. D Appl. Phys.* 42, 145409 (2009).
29. G. Joshi, H. Lee, Y.C. Lan, X.W. Wang, G.H. Zhu, D.Z. Wang, R.W. Gould, D.C. Cuff, M.Y. Tang, M.S. Dresselhaus, G. Chen, and Z.F. Ren, *Nano Lett.* 8, 4670 (2008).
30. Y. Ma, Q. Hao, B. Poudel, Y.C. Lan, B. Yu, D.Z. Wang, G. Chen, and Z.F. Ren, *Nano Lett.* 8, 2580 (2008).
31. NIST SRM 3451—Low Temperature Seebeck Coefficient Standard (10 K to 390 K) (2011).
32. N.D. Lowhorn, W. Wong-Ng, Z.Q. Lu, J. Martin, J.M.L. Green, E.L. Thomas, J.E. Bonevich, N.R. Dilley, and J. Sharp, *J. Mater. Res.* 26, 1983 (2011).
33. D.G. Cahill, K.E. Goodson, and A. Majumdar, *J. Heat Transf.-Trans. ASME.* 124, 223 (2002).
34. M. Maqsood, M. Arshad, and M. Zafarullah, *Supercond. Sci. Technol.* 9, 321 (1996).
35. W.J. Parker, R.J. Jenkins, C.P. Butler, and G.L. Abbott, *J. Appl. Phys.* 32, 1679 (1961).
36. H.S. Carslaw and J.C. Jaeger, *Conduction of Heat in Solids*, Oxford University Press, New York, 2nd ed. (1959), p. 101.
37. L.M. Clark and R.E. Taylor, *J. Appl. Phys.* 46, 714 (1975).
38. R.D. Cowan, *J. Appl. Phys.* 34, 926 (1963).
39. ASTM Designation E 1461, 933 (1992).
40. E.S.R. Gopal, *Specific Heats at Low Temperatures* (New York: Plenum, 1996), p. 9.
41. J.A. Koski, *Proceedings of the 8th Symposium of Thermophysical Properties*, Vol. II, 94 (1981).
42. R.C. Heckman, *Thermal Conductivity 14*, eds. P.G. Klemens, and T.K. Chu. Plenum, New York, 491 (1974).
43. J.A. Cape and G.W. Lehman, *J. Appl. Phys.* 34, 1909 (1963).
44. H. Wang, W.D. Porter, H. Böttner, J. König, L. Chen, S.Q. Bai, T.M. Tritt, A. Mayolet, J. Senawiratne, C. Smith, F. Harris, P. Gilbert, J. Sharp, J. Lo, H. Kleinke and L. Kiss, *J. Electron. Mater*. (2013). doi:10.1007/s11664-012-2396-8.